

Date: _____

EIC Detector R&D Progress Report

Project ID: eRD11 - simulation

Project Name: RICH Detector for the EIC's Forward Region PID

Period Reported: from January 1, 2015 to June 1, 2015

Project Leader: _____

Contact Person: _____

PROGRESS REPORT OF eRD11 PROJECT – RICH DETECTOR FOR THE EIC'S FORWARD REGION PARTICLE IDENTIFICATION

January 1 – June 15, 2015

The eRD11 Collaboration

Marcel Demarteau, Jingbo Wang, Robert Wagner
Argonne National Lab, Argonne, IL 60439

Jin Huang
Brookhaven National Lab, Riverhead, NY 11901

Xiaochun He, Murad Sarsour, Cheuk-Ping Wong, Liang Xue
Georgia State University, Atlanta, GA 30303

Marco Contalbrigo, Alessio Deldotto
INFN, Sezione di Ferrara, 44100 Ferrara, Italy

Fernando Barbosa, Jack McKisson, Yi Qiang,
Patrizia Rossi, Wenze Xi, Beni Zihlmann, Carl Zorn (co-PI)
Jefferson Lab, Newport News, VA 23606

Amaresh Datta, Douglas Fields
The University of New Mexico, Albuquerque, NM 87131

J. Matthew Durham, Hubert van Hecke (co-PI), Ming Liu
Los Alamos National Lab, Los Alamos, NM 87545

Zhiwen Zhao
Old Dominion University, Norfolk, VA 23529

William Brooks, Rodrigo Mendez
Universidad Tecnica Federico Santa Maria, Valparaiso, Chile

Abstract

The eRD11 R&D program is investigating the technology to be used for a Ring Imaging Cherenkov (RICH) detector for the hadron particle identification in the forward region of the future Electron-Ion Collider (EIC). Both the dual-radiator RICH option and a modular RICH concept are being investigated. This report covers the simulation component of the program.

Past

The proposal comprises two different RICH design options: the modular option, using only aerogel as a Cherenkov radiator, and the dual-radiator option, using both aerogel and a gas volume as radiators. In this review period, only the first option was explored, though work has started on the dual-radiator simulation studies.

A stand-alone version of the modular design had been implemented in GEANT4, and for this review period, the target was to take this design and integrate it into the larger EIC detector framework, and study the pattern recognition and particle identification capabilities.

The modular RICH consists of a Cherenkov radiator (aerogel), an acrylic Fresnel lens, and a photon detector, enclosed in a box with reflective walls, as shown in Fig. 1. The dimension of this unit is determined by the size of the available aerogel tiles, or by the size limitations of available fresnel lens, but is expected to be of the scale between 10 to 20 cm.

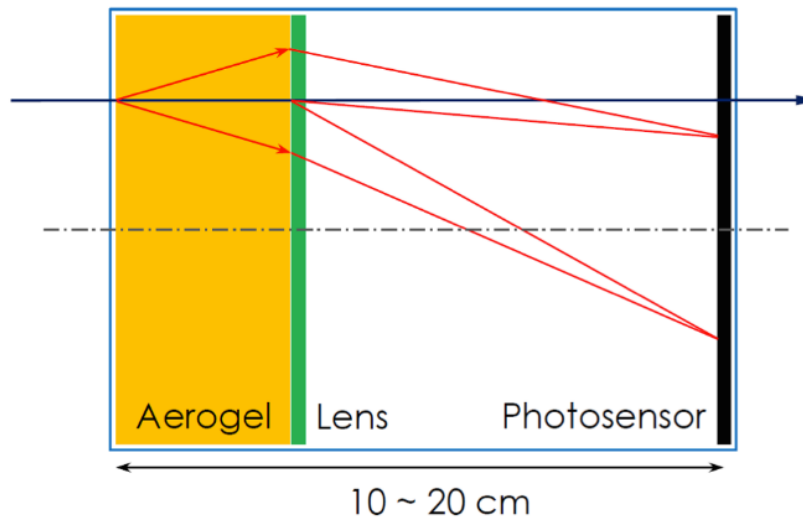


Figure 1: Diagram of a modular imaging aerogel detector, which consists of an aerogel radiator (orange), a Fresnel lens (green) and a photon detector (black). The dimension of the unit is between 10 cm to 20 cm.

Detector Simulation Setup

The simulation is built within the GEant4 Monte-Carlo (GEMC) simulation framework. Figure 2 shows the detector display of the modular RICH which consists of a block of aerogel (SiO_2) at the front as a radiator, followed by a fresnel lens, four sheets of light reflecting mirrors (top, bottom front, and back), and a photosensor plane at the end. Also shown in Fig. 2 are photons generated by 5 GeV mu-

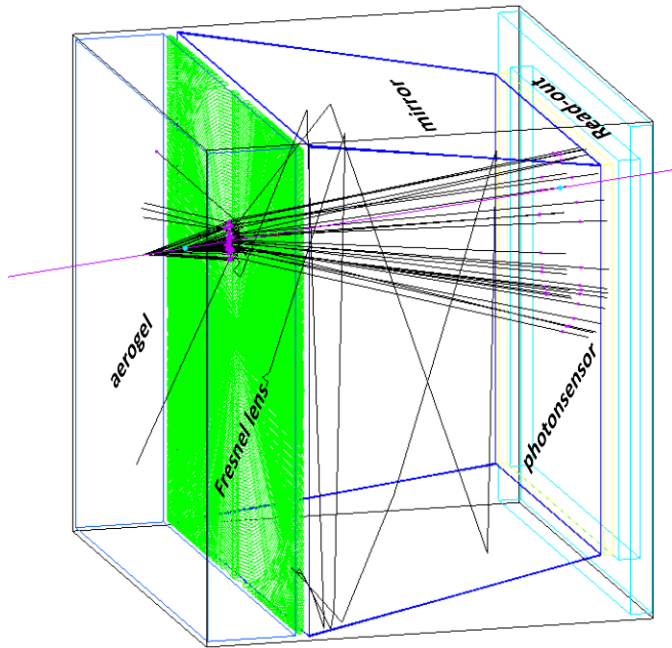


Figure 2: Implementation of a modular counter unit in GEMC framework. Visible are aerogel, fresnel lens, mirrors, photosensor, and read-out.

The optical properties of aerogel are crucial parameters for the performances of RICH detectors. The aerogel tile used in the modular RICH detector is 2 cm thick block which has a density of 0.02 g/cm^3 and a refractive index of $n=1.025$, and high clarity. The aerogel properties are typical of high-quality tiles currently available.

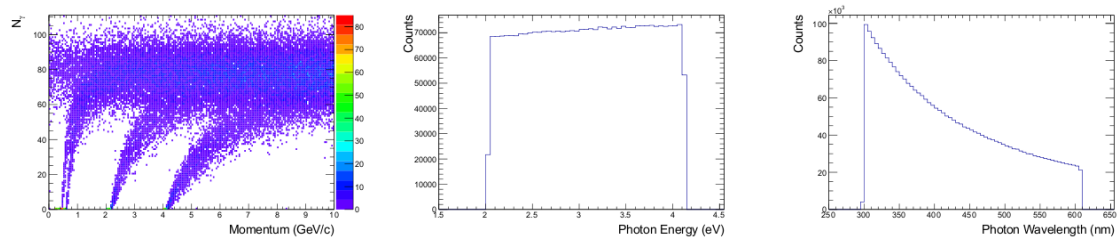


Figure 4: Left: Number of Cherenkov optical photons generated in radiator vs. the momentum of the incident particles (μ , π , K and p). Middle: Energy distribution for Cherenkov optical photons in the aerogel. Right: Wavelength distribution for Cherenkov optical photons in the aerogel.

The fresnel lens in the simulation is made of acrylic, with 100 concentric grooves. It was optimized to have a very short focal length relative to its diameter, in order to keep the ring image smaller than the modular unit transverse dimension. The acrylic is not transparent to UV photons. However, UV photons are the most likely to Rayleigh scatter in the aerogel, and would cause background hits in the detector plane. The lens therefore also functions as a filter to reduce out-of-ring background hits. As a result, the photosensor plane in this design should be sensitive in the visible part of the spectrum, $\sim 300\text{-}500 \text{ nm}$.

The dimensions of the photosensor plane are $88 \times 88 \text{ mm}$, which is in this study segmented into 1 mm square readout pads. Three types of photosensor materials are considered for the photosensor plane: bialkali crystals, GaAs, and GaAsP. These materials have relatively high quantum efficiencies (see Fig. 5), but different frequency responses.

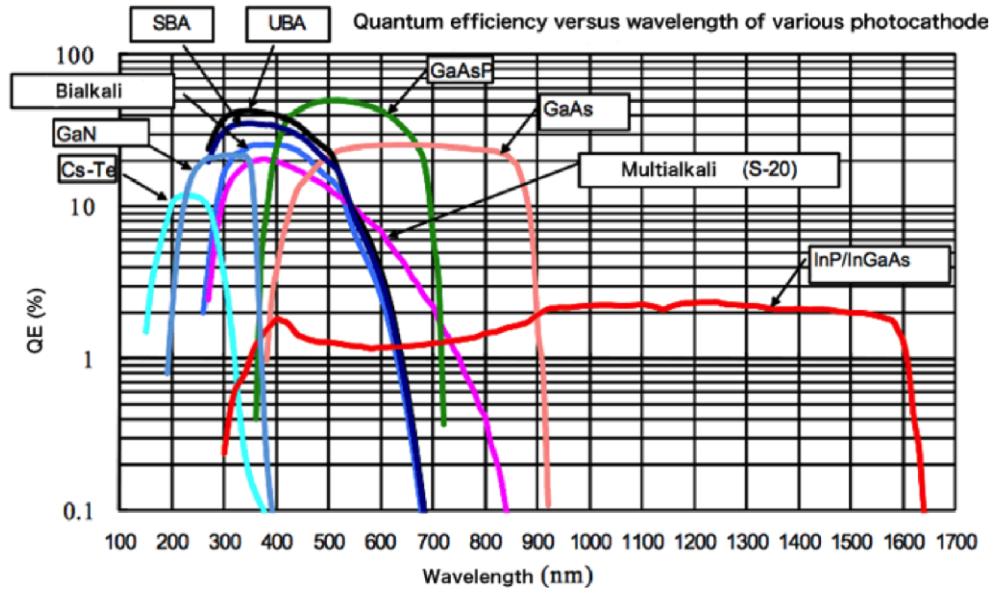


Figure 5: Comparison of quantum efficiency curves with various photocathode materials (from Hamamatsu Photonics Corporation).

Figure 6 shows simulated photoelectron production for bialkali crystal (Sb-Cs-K) and semiconductor materials (GaAs, GaAsP). Typically, 5 GeV muons passing through the detector can produce 5 electrons for Sb-Cs-K, 11 electrons for GaAsP, and 3 electrons for GaAs.

In order to study the effects of the detector nonuniformity (imperfect aerogel and/or lens), we smear the photon hit position using a 2-D Gaussian distribution at the photon sensor plane. An example of the smearing is given in Fig. 7. The left panel Fig. 7 shows a ring form generated by a 5 GeV muon before the smearing of the photon hit position. The middle panel shows the ring form after the position smearing. The right panel shows the ring form with additional quantum efficiency correction after the hit position smearing applied.

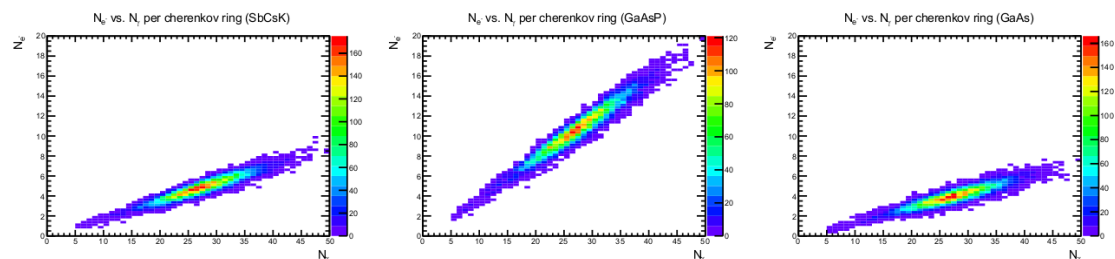


Figure 6: Photoelectron production as a function of number of optical photons for bialkali crystals Sb-Cs-K (left panel), and semiconductor materials such as GaAsP (middle panel) and GaAs (right panel).

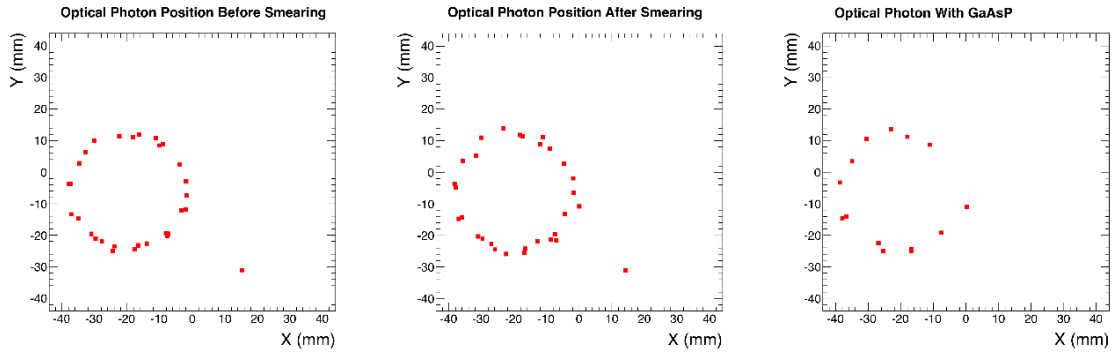


Figure 7: Left: Cherenkov radiation ring before photon position smearing. Middle: Cherenkov radiation ring after photon position smearing. Right: Cherenkov radiation ring after photon position smearing and with photosensor material quantum efficiency applied.

Particle Identification Algorithms

Ring Finder using Hough transforms

A ring finder algorithm using a Hough transform method is developed to identify the Cherenkov radiation rings on the photosensor plane [4]. This algorithm performs a transformation from the image space to the parameter space. Any three detected photon-electron positions on the photosensor plane defines a ring. The combinatorial of the rings determined from the transforms will give an enhancement at the real ring center in the image space. Figure 8 shows the Cherenkov rings on the photosensor plane generated by two muons. The ring centers and radii are calculated using the combinatorial Hough transform and are given in Fig. 9.

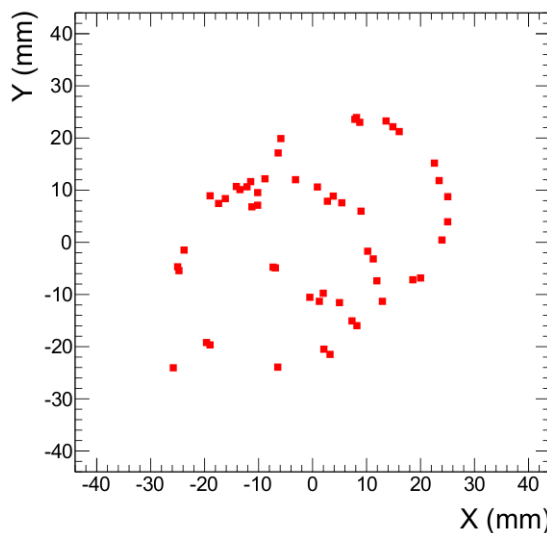


Figure 8: Cherenkov rings on the photosensor plane generated by two muons.

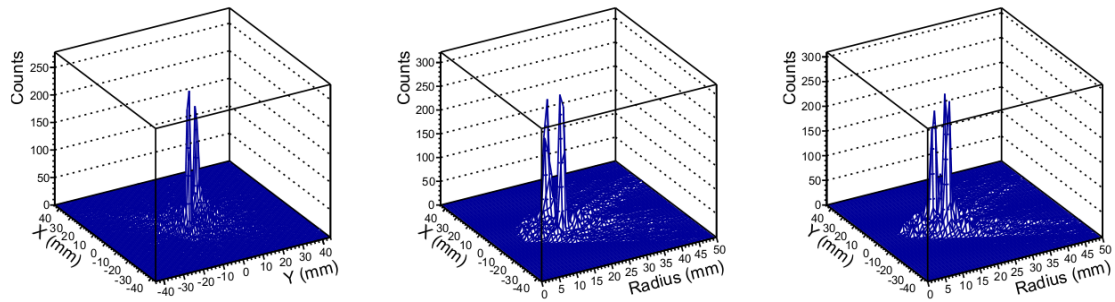


Figure 9: Left: Cherenkov radiation rings center calculated by combinatorial Hough transform; Middle: X position and Cherenkov radiation ring radius calculated by combinatorial Hough transform; Right: Y position and Cherenkov radiation ring radius calculated by combinatorial Hough transform;

Maximum Likelihood Method

The maximum likelihood technique has been used for particle identification in many experiments [5]. It is based on the fact that the detector response for different particle species are different at a given momentum. The number of photoelectrons n_{el} in each $1 \times 1 \text{ mm}^2$ pixel follows a Poisson distribution. For studying the noise level response of the photosensor plane, two photoelectrons are randomly added to the hit list across the entire 88×88 sensor cells.

PID Performance for Single Particles

Using Ring Finder Algorithm

1000 single electrons, μ^- , π^- , K^- and protons are launched 5 cm away from the aerogel with incident angles ranging $\pm 15^\circ$ in theta and 2π in phi (non-reflected rings) to study the detector performance using ring finder algorithm. The particle momenta range from 0 to 10 GeV/c. Figure 11 shows an example of the calculated rings with the photosensor materials of SbKCs (left panel), GaAs (middle panel), and GaAsP (right panel) for a 5 GeV/c muon.

The calculated ring radii as a function of particle momentum are shown in Fig. 12. The left panel in Fig. 12 is the ring radius for the SbKCs photosensor material, the middle panel is for GaAs and the right is for GaAsP. It is clear to see that in order to achieve better PID performance, a higher quantum efficiency material for the photosensor plane is needed (as seen in the bottom panel of Fig. 12).

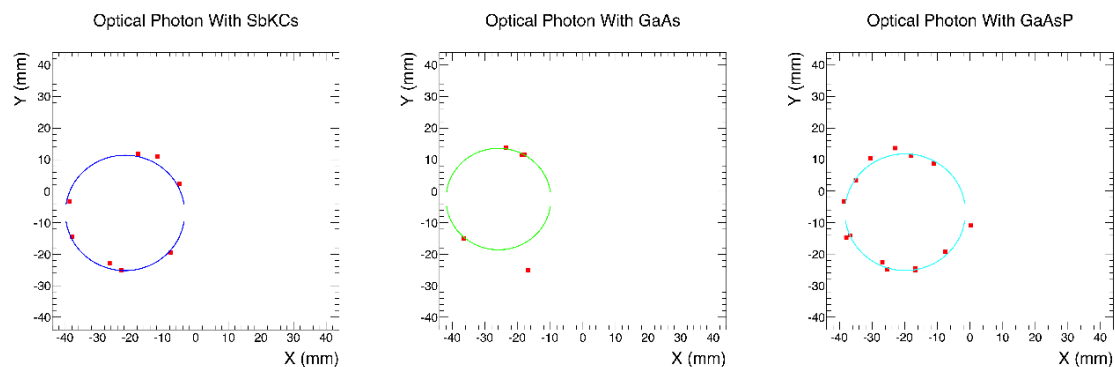


Figure 11: A example of rings finder for single muon with material SbKCs (left), GaAs (middle), and GaAsP (right).

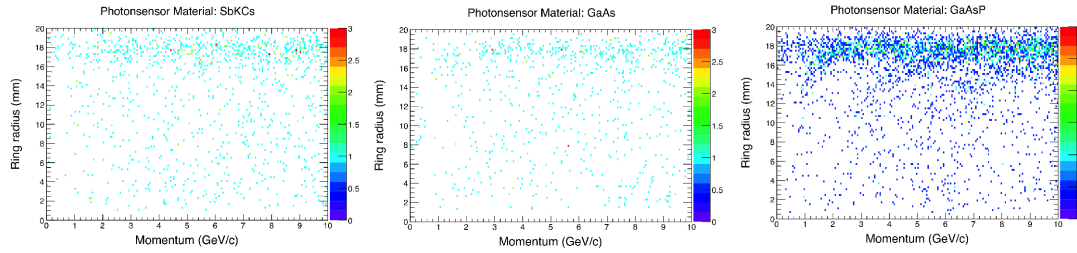


Figure 12: Calculated ring radius as a function of momentum with material SbKCs (left), GaAs (middle), and GaAsP (right), using the Hough transform method.

The Hough transform method relies on the assumption that the ring images formed in the detector plane are (sections of) circles. For a lens with a small focal-length-to-diameter ratio, this is not a valid assumption for off-axis incident particles. Therefore this method is no longer pursued.

Using Maximum Likelihood Method

For this study, 1000 pions, kaons and protons are simulated at each momentum (ranging from 3 to 15 GeV/c with 0.2 GeV/c step size) with incident theta angle at 5° , 25° , 45° , and phi angle equal to 45° for generating the single particle response distribution. Figure 13 shows a series of event displays of 5 GeV/c muons at incident theta angle at 5° , 25° , 45° from left to right, respectively. At an incident angle of 45° , all of Cherenkov photons are gone through a mirror reflection.

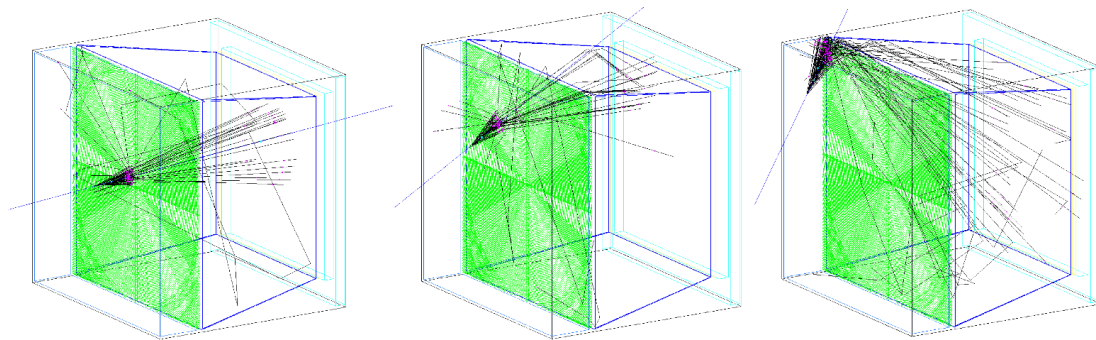


Figure 13: Event display of 5 GeV/c muons at incident theta angle at 5° , 25° , 45° . At higher incident angles, some or all of the photons undergo a reflection off the units mirrored walls.

The single particle response distributions are shown in Fig. 14. These simulations form a database that is subsequently used in the analysis, to identify particles by comparison to the patterns in the databases.

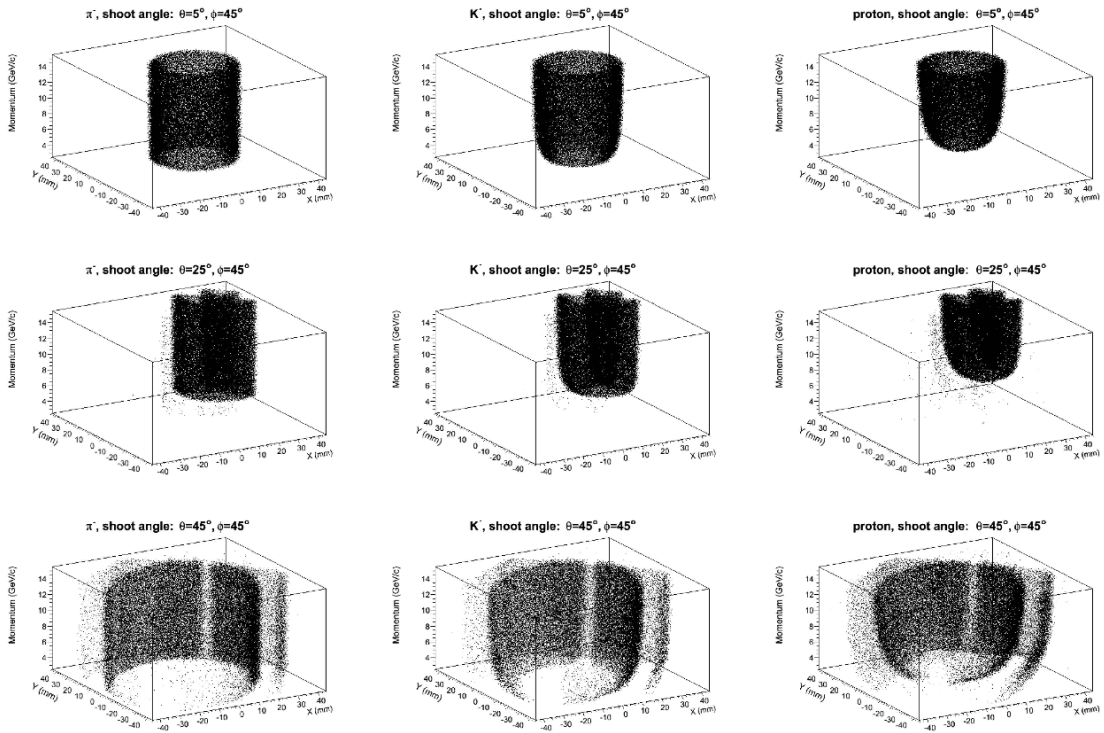


Figure 14: The single particle response distributions which form the database for applying the maximum likelihood method.

Figures 18, 19, 20 show the (mis)identification probabilities for pi, K, p using the database built up with the simulations.

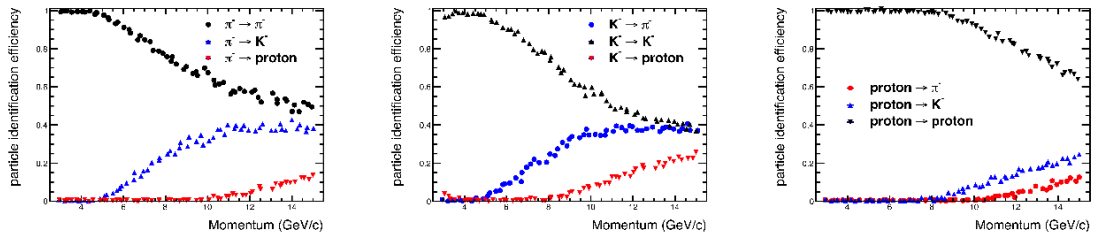


Figure 18: Theta 5 Phi 45

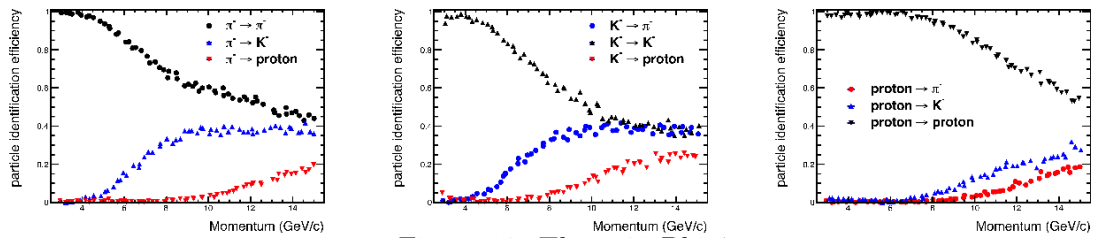


Figure 19: Theta 25 Phi 45

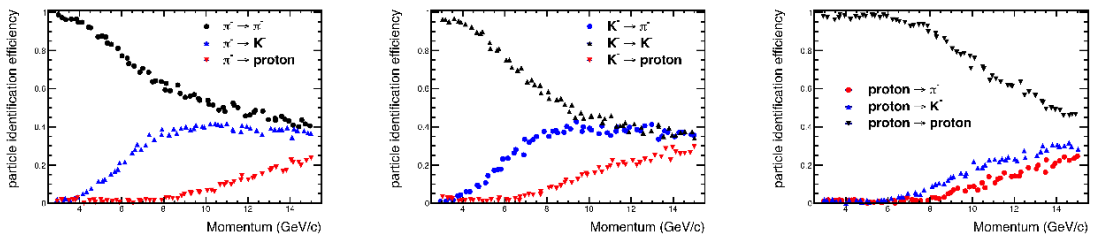


Figure 20: Theta 45 Phi 45

Identification works well at low momenta, but becomes less efficient at higher

momenta. Varying the aerogel index of refraction can be studied in an effort to extend the particle ID range.

Plan on PID Performance for multiple Particles

In high multiplicity or jetty EIC events, multiple particles could enter the same RICH module. Our analysis packages are in good shape to expand analysis into handling such situations. As shown in Figure 11, the ring finder algorithm can already handle two rings. Meanwhile the likelihood package can accommodate two candidate templates (as shown in Figure 14) together, in order to analyze the double ring cases. The performance will be quantified in comparison to the single particle cases.

Integration with a realistic EIC environment

We are considering testing our design and analysis packages in possible full EIC detector designs and full event EIC environment.

MEIC Detector

Work has begun on building up a full-scale detector array using the modules. Figure 23 shows a large number of modules stacked to make a thin PID wall.

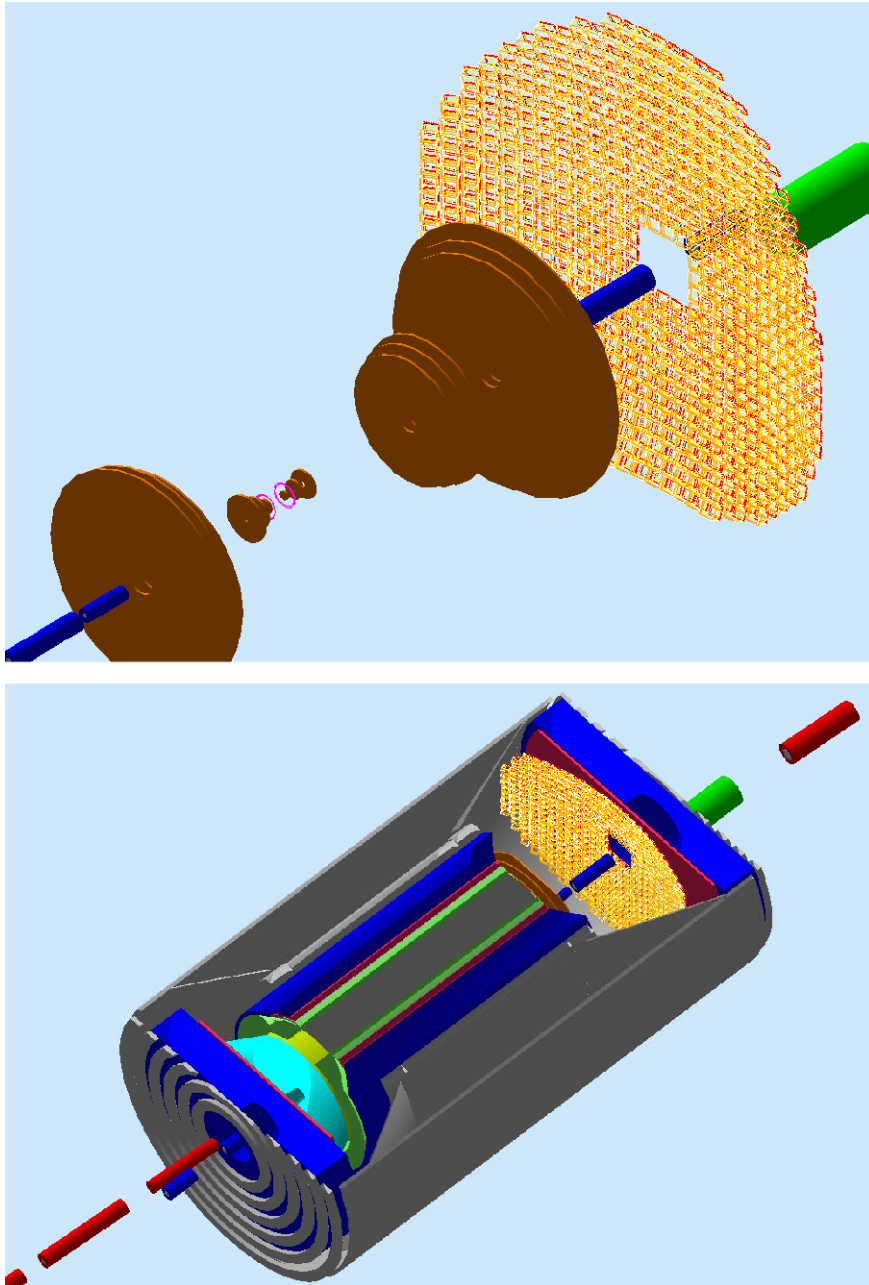


Figure 23: Modular RICH detectors integrated in MEIC.

Plan to use in other EIC detector designs

With one possible detailed layout demonstrated in the MEIC forward spectrometer, we can further test the concept of modular RICH in other full EIC detector concepts in a faster way. For example, the modular RICH design fit well in to the ePHENIX detector design as the aerogel RICH detector [5]. Rather than redo the RICH wall layout in the ePHENIX detector, we will record the particle flux through the aerogel RICH detector as in the full event full detector ePHENIX simulation, inject the particle flux into our standalone modular RICH simulation and analyze in our likelihood package. Through such study, we plan to demonstrate the wide applicability of our design in multiple concepts of EIC detectors, as well as provide

feedback on tracking and magnetic field design to the full detector concept developers.

Future

The simulation work on the modular design is envisioned to continue at the present level of effort. The properties of the aerogel and acrylic lens can be tuned to optimize the PID efficiencies. Now that the modules have been tiled into an array in the larger EIC detector, the capabilities of the array of Cherenkov modules can be explored with full event simulations. The pythiaRICH 1.0 event generator has been installed for this purpose.

The dual radiator concept requires a separate effort. Recently, an INFN postdoc has picked up this project, and he will be available full-time for 6 months.

Manpower

Liang Xue (GSU) was funded through EIC R&D. The studies reported here were performed by Liang Xue, postdoc at Georgia State (at approximately 50%), working with prof. Xiaochun He. Hubert van Hecke (Los Alamos) and Jin Huang (BNL) also advised. Cheuk-Ping Wong (Georgia State) played a supporting role, being familiar with GEMC framework. Zhiwen Zhao (JLab) was instrumental for helping Liang to get started with the GEMC simulation.

On May 15, Alessio Deldotto joined the simulation effort (100%), specifically to study the gas RICH and dual rich configurations. He is funded by the generic EIC R&D eRD11, through JLab to INFN.

External Funding

Staff members at LANL, BNL, JLab are participating free of charge.

Publications, Talks and References

‘Simulation Study of RICH Detector for Particle Identification in Forward Region at Electron-Ion Collider’, Cheuk-Ping Wong (Georgia State University), APS April Meeting 2015, Volume 60, Number 4, April 11-14, 2015, Baltimore, Md.

References

[1] http://p25ext.lanl.gov/~hubert/eic_rich/modular/agerl_sim.html

[2] <http://gemc.jlab.org>

[3] https://eic.jlab.org/wiki/index.php/EIC_Software

[4] http://en.wikipedia.org/wiki/Hough_transform

[5] PHENIX Collaboration, Concept for an Electron Ion Collider (EIC) detector built around the BaBar solenoid. arXiv:1402.1209 [nucl-ex]

[6] <https://github.com/EIC-eRD11>

